Behavior of panel zone with circular hollow section in steel beam-column joint under large deformation

Y.Ashida[1], Y. Koetaka[2], T. Nakano[3]

[1] Graduate student, Kyoto University, st.ashida@archi.kyoto-u.ac.jp
[2] Professor, Kyoto University, koetaka@archi.kyoto-u.ac.jp
[3] Associate professor, Utsunomiya University, nakanot@cc.utsunomiya-u.ac.jp

Abstract

It is well known that panel zones at beam-column joints of steel moment resisting frames (MRFs) exhibit stable elasto-plastic hysteresis characteristics and have large plastic deformation capacity. It has also been pointed out that the panel hinging mechanism is desirable because the damages are distributed into the entire structure as well as the beam hinging mechanism. Based on these knowledges, it can be thought that considering the panel zones yielding to the seismic design is effective to enhance efficiently the seismic performance of steel MRFs.

In Japan, bidirectional MRFs, in which beams are connected to columns with the closed section in orthogonal directions, are commonly applied. Previous studies have examined the behavior of subassemblies with rectangular hollow sectional columns and panel zones. However, few studies have been conducted on those with circular hollow sections. Based on the above background, this paper aims to clarify the effect of loading direction on large deformation behavior of weak panel type subassemblies, which consist of circular hollow section columns and bare H-shaped beams.

In the cyclic loading test, two same subassemblies were loaded in 0-degree and 45-degrees, respectively. The test was continued until some distinguished failures were observed up to 0.08 rad drift angle. Through the test results, it was revealed that the beams kept elastic against both the 0-degree and 45-degrees loading, and the columns yielded almost at the same time the panel zone yielded. In the case of 0-degree loading, strength deterioration occurred when the drift angle reaches 0.08 rad by a ductile fracture at the top edge of fillet weld between the panel zone and beam web. On the other hand, in the case of 45-degrees loading, ductile fracture at the toe of the full-penetrated weld between the panel zone and the through diaphragm was observed, and the strength deterioration occurred earlier than 0-degree loading. Further, under 45-degrees loading, the ratio of energy dissipation of panels was smaller and that of columns was larger than those under 0-degree loading. This can be attributed to the fact that the panel strength under 45-degrees loading is larger than that under 0-degree loading. Moreover, regardless of the loading direction, the cumulative plastic deformation until the strength of specimens was reduced to 90% of the maximum strength was greater than 1.0 rad, which was well above the required plastic deformation capacity of the panels described in previous study.

Keywords: steel structure, bidirectional cruciform subassembly, panel zone, loading direction, cyclic loading test

1. Introduction

It is well known that panel zones at beam-column joints of steel moment resisting frames (MRFs) exhibit stable hysteresis characteristics and have a large plastic deformation capacity[1][2]. It was also shown that the panel zone yielding leads to the desired collapse mechanism where the damages are distributed to the entire structure, similar to the beams yielding[2]. Based on the above background, a seismic design method that takes into account the panel zones yielding can achieve effectively enhancing the seismic safety of steel MRFs.

In Japan, bidirectional MRFs, in which beams are joined to columns with closed sections in two orthogonal directions, are commonly used. There are some previous studies[3-5] which have examined the behavior of subassemblies with rectangular hollow section column. However, few studies[3], [6-7] have been conducted on those with circular hollow section columns. Moreover, most of the studies on subassemblies with circular hollow section columns assumed that the horizontal force is applied in a direction parallel to structures. Since MRFs may be subjected to bidirectional horizontal forces during earthquakes, the effect of loading direction on behavior of weak panel type subassemblies should be figured out. However, loading tests on subassemblies with circular hollow columns subjected to bidirectional loading are limited to only two cases in Ref. [7] and have not been sufficiently investigated.

Furthermore, in the case of weak panel type subassemblies, which consist of circular hollow section columns and H-shaped beams, the ultimate states have only been confirmed in some of the experiments in Ref. [6]. Therefore, it is still necessary to provide additional information about the elasto-plastic behavior and ultimate state of circular tube panel.

This paper aims to examine the effect of loading direction on behavior of weak panel type subassemblies, which consist of circular hollow section columns and H-shaped beams. Based on the objectives, cyclic loading test was conducted using subassemblies with through diaphragms, where the yielding of the panel zones precedes that of the other members. Since there are only a limited number of tests confirming the ultimate state of such subassemblies as described above, in this test, loading is continued until the strength of the specimens deteriorates.

2. Experimental program

2.1 Test specimens

Fig. 1(a) shows the geometry and details of the test specimens. They represent the interior beam-column subassemblies extracted from steel moment frame, assuming that the inflection points are at the mid-point of all the components. To accommodate the capacity of the loading facility, the specimens were fabricated at 2/3 scale in geometric dimension. The experimental parameter is the loading direction, which is 0-degrees parallel to plane of the frame and 45-degrees to plane of the frame, as shown in Fig. 1. In this research, for Specimen CPB_17, a single oil jack was employed to provide a force in 45-degrees direction to orthogonal planes of the frame.

Two identical specimens shown in Fig. 1(a) were fabricated for the test. Fig. 1(b), (c) and (d) show details about beam-to-column connection. Two diaphragm plates were inserted between columns and panel. The thickness of diaphragm plate was 19 mm, which was much thicker than beam flanges. The diaphragm plates were extended from the column face by 21.3 mm. The beam flanges, columns and panel were welded to the diaphragm by complete-joint-penetration groove welds, and the beam webs were welded to panel by fillet welds. The weld access holes were adopted to enable the welding construction convenient to operate, the shape of which was recommended by Japanese Specification[8]. The rectangular backing bars were used at the location of welding to secure firm welding quality.

Table 1 lists the sectional dimension and steel grade of each member for all the specimens. The beam depth and the diameter of panel zones were selected to be near the upper limit of the panel aspect ratio to which the full-plastic moment formula of panel zones in Ref. [2] can be applied. In addition, the cross-sectional dimensions of column and beam were defined with the intention that the yielding of the panel should precede those of the other members. As a result, the panel aspect ratio d_b/d_c is 1.7, as illustrated in Fig. 1(c).

2

Table 1 also shows the lateral forces required to cause the specimens to reach their beam plastic moment ($_bM_p$), column plastic moment ($_cM_p$) and panel plastic shear strength ($_pQ_p$), as illustrated in Fig. 2. The lateral forces were calculated through following equations:

$$_bQ^* = \frac{2\,_bM_p}{(1 - d_c/L)H} \tag{1}$$

$$_cQ^* = \frac{2\,_cM_p}{H - d_b} \tag{2}$$

$$_pQ^* = \frac{_pQ_p d_b}{(1 - d_c/L - d_b/H)H} \tag{3}$$

in which L and H denote the distances between the inflection points of adjacent beams and columns, respectively. Beam plastic moment $_bM_p$, column plastic moment $_cM_p$ and panel plastic shear strength $_pQ_p$ are calculated using the measured yield strength of steel and thickness of test pieces shown in Table 2. Note that $_pQ_p$ is calculated according to Ref. [2], and $_cM_p$ and $_pQ_p$ are projected onto plane of the frame, which is the direction parallel to the beam.
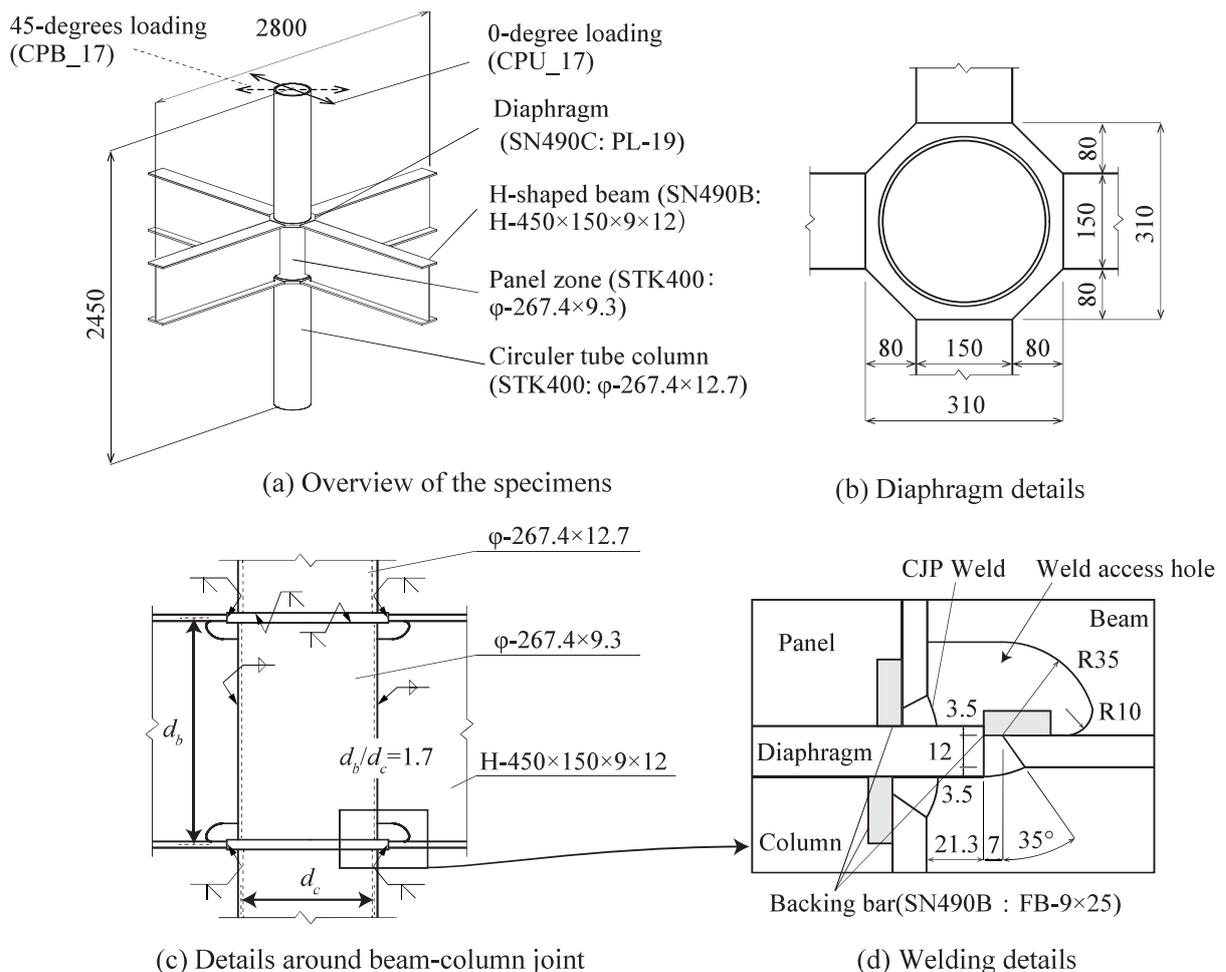

(a) Overview of the specimens

(b) Diaphragm details

(c) Details around beam-column joint

(d) Welding details

Fig. 1 – Test specimens

Table 1 – Test specimen

Spec. name	Loading direction	Cross-sectional dimension (unit: mm)			Lateral force to cause components yield				
		Panel (STK400)	Column (STK400)	Beam (SN490B)	$_pQ^*$ (kN)	$_cQ^*$ (kN)	$_bQ^*$ (kN)	$_cQ^*/_pQ^*$	$_bQ^*/_pQ^*$
CPU_17	0-degree	φ-267.4 ×9.3	φ-267.4 ×12.7	H-450×150 ×9×12	232	248	403	1.07	1.73
CPB_17	45-degrees				164	175			2.45

Note: Strengths are calculated based on the pre-measured thickness and yield strengths in Table 2.

Table 2 – Mechanical properties of steel

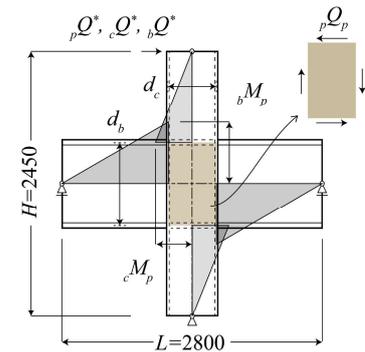| Location		Thickness (mm)	Steel grade	Yield strength (N/mm²)	Ultimate strength (N/mm²)	Elongation at fracture (%)
Beam	Flange	12.0	SN490B	381	515	25.6
	Web	9.1		349	506	24.5
Column		12.1	STK400	319	425	39.8
Panel		8.9		357	444	35.8

Fig. 2 – Moment diagram

2.2 Test setup, measurement arrangement and loading protocol

Fig. 3 shows the test setup and measurement arrangement. The column ends were pin-connected to the foundation beam and the oil jack, and the center-to-center length between the pins was 2450mm. The beam ends were supported by the links which were attached with spherical hinges to permit free rotation in any direction and were at a distance of 1400 mm away from the centerline of the column. The lateral support system was provided to prevent out-of-plane deformation and twisting of specimen during test.

The measurement was carried out by 3D image measurement system using CMOS cameras and displacement transducers as shown in Fig. 3. CMOS cameras shot only the area around the beam-column joint, while the displacement transducers were set on far away from the connection.

Cyclic loading was controlled by drift angle R in the direction of the frame parallel to the beam. The loading amplitude was repeated once at 0.004 rad, then twice at 0.02 rad, 0.04 rad, 0.06 rad and 0.08 rad increasing by 0.02 rad. The test was continued until some distinguished failures were observed up to 0.08 rad drift angle.
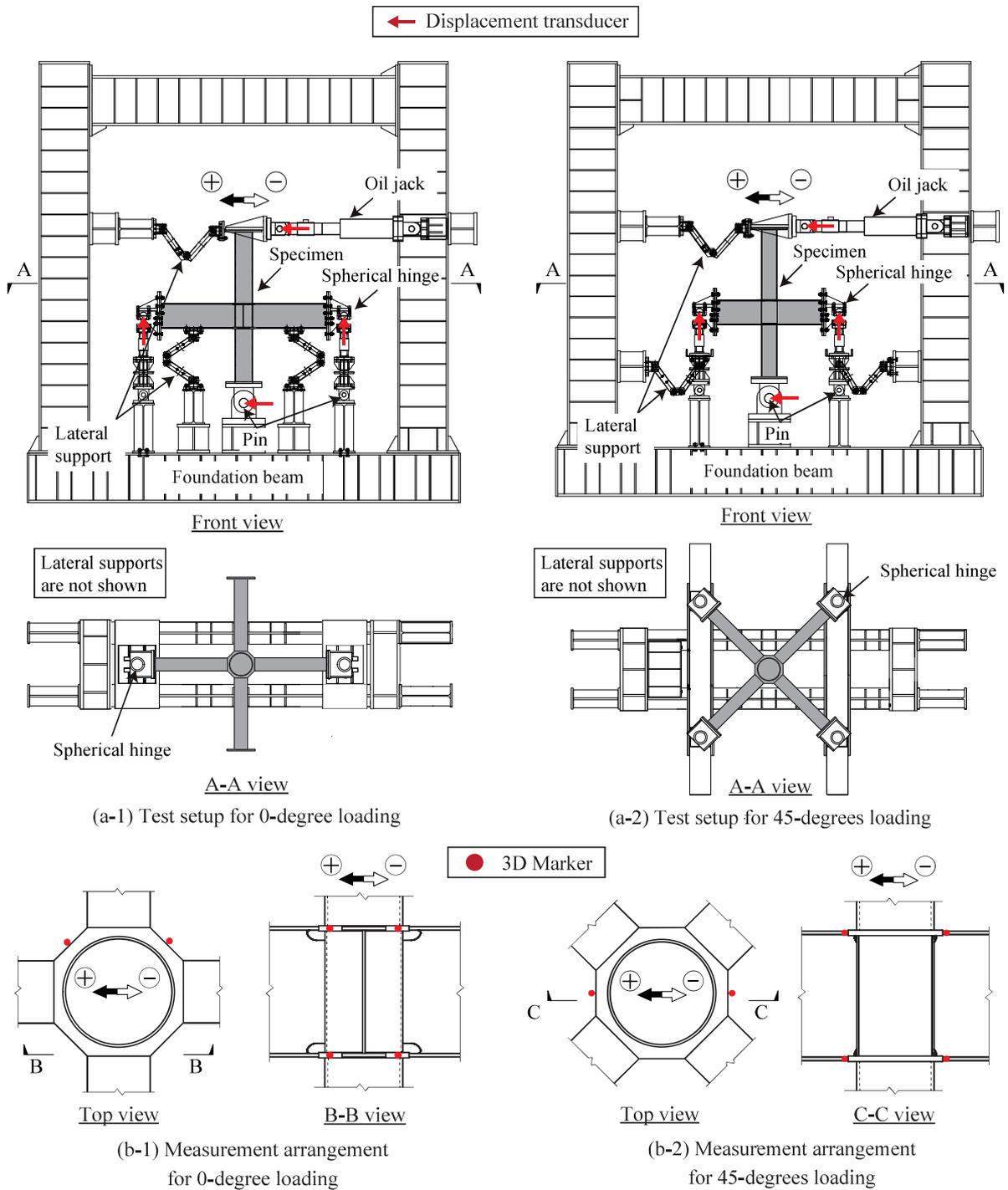
← Displacement transducer

Oil jack

Specimen

Spherical hinge

A ─── A

Lateral support

Pin

Foundation beam

Front view

Lateral supports are not shown

Spherical hinge

A-A view

(a-1) Test setup for 0-degree loading

Oil jack

Specimen

Spherical hinge

A ─── A

Lateral support

Pin

Foundation beam

Front view

Lateral supports are not shown

Spherical hinge

A-A view

(a-2) Test setup for 45-degrees loading

● 3D Marker

+ −

B ─── B

Top view

B-B view

(b-1) Measurement arrangement
for 0-degree loading

+ −

C ─── C

Top view

C-C view

(b-2) Measurement arrangement
for 45-degrees loading

Fig. 3 – Test setup and measurement arrangement

5

3. Experimental results

3.1 Hysteresis curve and failure mode

Fig. 4 shows the hysteresis curves between nodal moment M^* and drift angle due to each member. The nodal moment M^* represents the sum of the moments of each member at the cross point of the centerlines of beams and columns, and is calculated by the following equation:

$$M^* = \frac{{}_bM_r + {}_bM_l}{1 - d_c/L} = \frac{{}_cM_u + {}_cM_l}{1 - d_b/H} = \frac{{}_pM}{1 - d_b/H - d_c/L} \tag{4}$$

where ${}_cM_u$, ${}_cM_l$ are the bending moment acting at the end of the upper and lower columns, ${}_bM_r$, ${}_bM_l$ are the bending moment acting at the end of the right and left beams, respectively. The panel moment ${}_pM$ is obtained by the following equation:

$$_pM = {}_bM_r + {}_bM_l - \frac{d_b}{2}\left({}_cQ_u + {}_cQ_l \right) \tag{5}$$

where ${}_cQ_u$, ${}_cQ_l$ are the shear force acting on the upper and lower columns, respectively. Note that the moment and drift angle are projected onto the plane of the frame. ${}_pR$, ${}_cR$, and ${}_bR$ are the components of the drift angle of the panel, column, and beam, and the sum of these components is almost identical with the total drift angle.

For specimen CPU_17, strength deterioration was observed during the first positive loading cycle of 0.08 rad. This was due to a ductile fracture at the toe of the weld between the panel flange and the beam web on the oil jack side, which propagated about 6-degrees in the panel circumferential direction. Here, this crack was first observed at negative peak rotation of the second cycle of 0.04 rad. Subsequently, a ductile fracture initiated at the weld edge between the panel flange and the beam web on the opposite side of the oil jack (Fig. 5 (a): Crack initiation point) propagated in the circumferential direction of the panel during positive loading of 0.08 rad, causing the strength of the specimen to decrease to 90% of the maximum strength. The above cracks first occurred at negative peak rotation of first cycle of 0.04 rad.

Moreover, a ductile fracture propagating from the bottom of the weld access hole penetrated the beam flange in the thickness direction (Fig. 5 (a): Crack penetration), even though the plastic deformation of the beam was quite small, as shown in Fig. 4. This is considered to be due to the out-of-plane deformation of the beam flange at the joint position between the beam flange and the beam web caused by the crack propagation in the panel in Fig. 5 (a).

For specimen CBU_17, strength deterioration was observed during the second negative loading cycle of 0.06 rad. This was due to the circumferential propagation of a ductile fracture at the toe of weld between the panel flange and the upper diaphragm on the opposite side of the oil jack. During the 0.08 rad first cycle of positive loading, the crack at the bottom of the weld end on the panel side between the panel flange and the lower diaphragm on the opposite side of oil jack, which occurred at positive peak rotation of the second cycle of 0.04 rad, propagated in the panel circumferential direction (Fig. 5 (b)). In this case, local buckling due to bending moment was slightly observed in the panel flange, which was not observed in the panel flange of CPU_17.
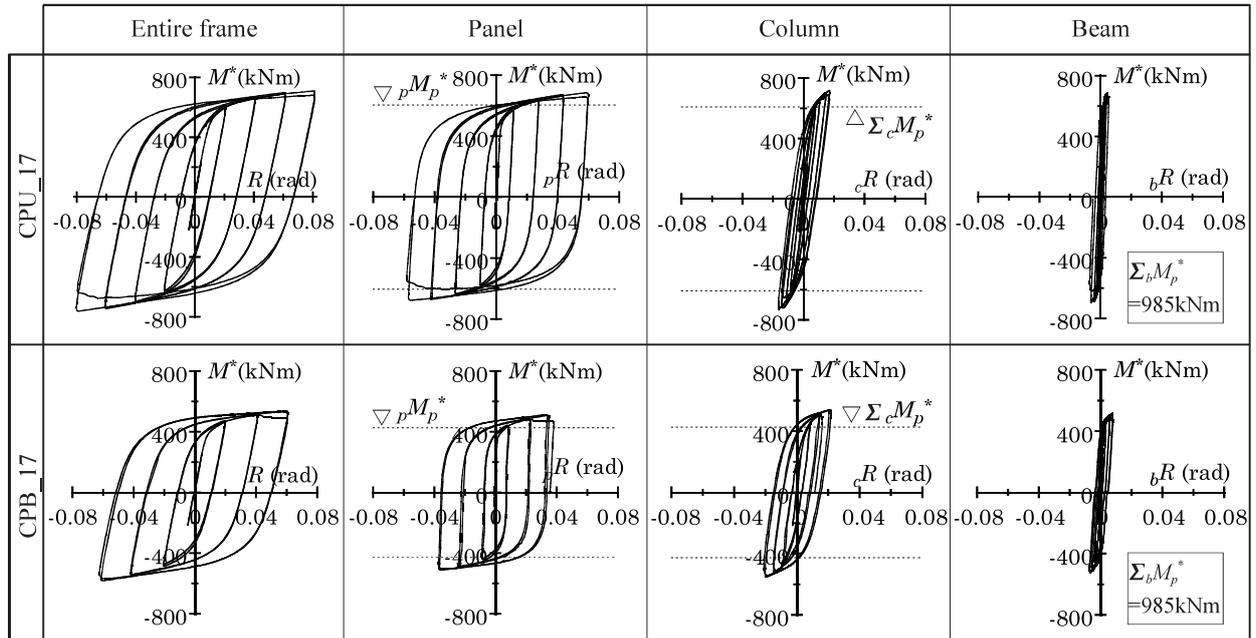
6

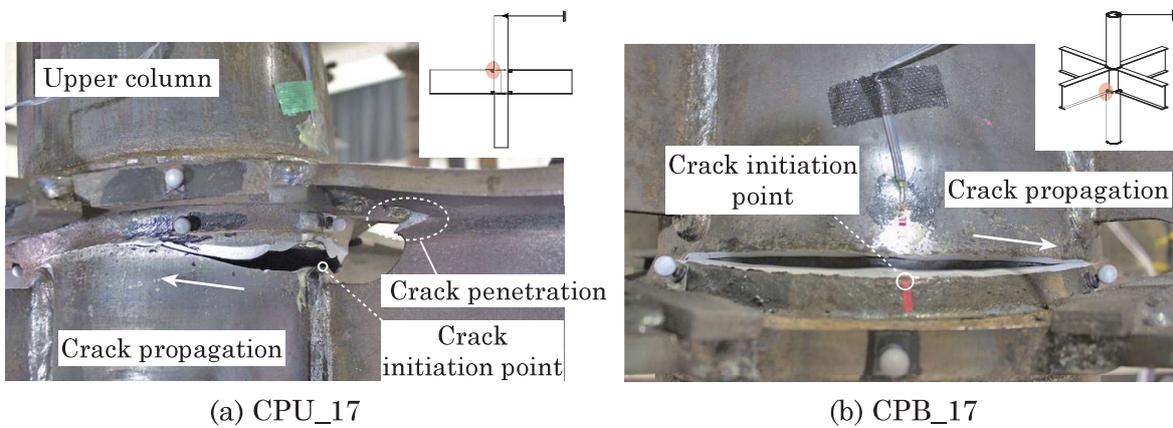Fig. 4 – Hysteresis curve (projected onto plane of the frame)

(a) CPU_17 (b) CPB_17

Fig. 5 – Ultimate state of specimens

3.2 Energy dissipation ratio of each member

Fig. 6 shows the ratios of cumulative dissipated energy by each member to the total cumulative energy by the entire frame for each loading cycle after 0.02 rad, when the first yielding of the member was observed. Fig. 6 shows that, the ratio of energy dissipation by the panel of CPB_17 was smaller, and the ratio of energy dissipation by the columns was larger than those of CPU_17.
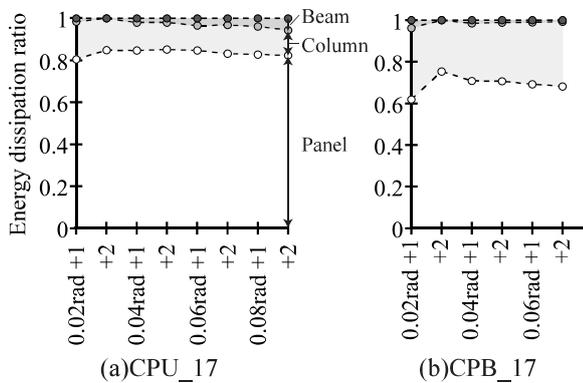
(a)CPU_17   (b)CPB_17

Fig. 6 − Energy dissipation ratio of each members

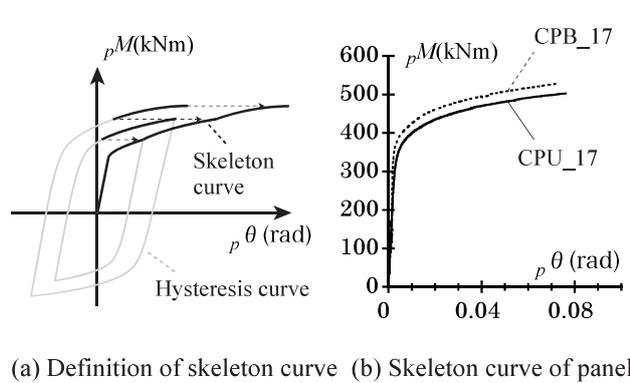(a) Definition of skeleton curve   (b) Skeleton curve of panel

Fig. 7 − Skeleton curves of panel

3.3 Elasto-plastic behavior of panel zones

Fig. 7 shows the skeleton curve of the panel based on the panel moment $_pM$ − panel deformation angle $_p\theta$ relationship projected onto the loading direction.

As discussed in Section 3.2, compared to the case of 0-degree loading, the ratio of dissipated energy by the panel decreases and the ratio of dissipated energy by the columns increases in the case of 45-degrees loading. This can be attributed to the fact that, as shown in Fig. 7, the bearing capacity of the panel in the case of 45-degrees loading is slightly greater than that in the case of 0-degree loading.

The cumulative plastic deformation until the bearing capacity of the panel was reduced to 90% of the maximum strength was 1.31 rad for CPU_17 and 1.09 rad for CPB_17. These values were well above the required plastic deformation capacity of the panels given in Ref. [9].

4. Conclusions

In this paper, taking loading directions as an experimental parameter, cyclic loading test was conducted using weak panel type subassemblies, which consist of circular hollow section columns and H-shaped beams. Further, differences in the elasto-plastic behavior of the subassemblies depending on the loading direction were examined based on the test results. The major findings are summarized as follows.

1. Under 0-degree loading, the strength of the specimen deteriorated due to ductile fracture initiated at the edge of the weld between the panel flange and the beam web. On the other hand, under 45-degrees loading, the test specimen was deteriorated due to ductile fracture at the edge of the weld on the panel side between the panel flange and the through diaphragm.

2. Under 45-degrees loading, the ratio of energy dissipation by panel was smaller and that by columns was larger, than those under 0-degree loading. This can be attributed to the fact that the panel strength under 45-degrees loading is slightly larger than that under 0-degree loading.

3. Regardless of the loading direction, the cumulative plastic deformation until the strength of specimens was reduced to 90% of the maximum strength was greater than 1.0 rad, which was well above the required plastic deformation capacity of the panels described in Ref. [9].

8

Acknowledgements

References

[1] AISC: *Seismic Provisions for Structural Steel Buildings*, American Institute of Steel Construction, 2016.7

[2] AIJ: *Recommendation for Design of Connections in Steel Structures*, Architectural Institute of Japan, 2012.3(in Japanese)

[3] Kuwahara, S., and Inoue, K.: The shear force loading test for the beam-to-column joint panels of rectangular and circular hollow section, *Journal of Structural and Construction Engineering* (*Transactions of AIJ*), No.502, pp.149-156, 1997.12 (in Japanese)

[4] Namba, H., Tabuchi, M., Tanaka,T., Kitaoka, S.: Behaviour on tapered joint panels in RHS column to beam connections, *Journal of Structural and Construction Engineering* (*Transactions of AIJ*), Vol.69, No. 579 , 2004.5, pp. 95-102, (in Japanese)

[5] Wang, Y., Arakida, R., Chan, I., Koetaka, Y., Nakano, T.: Cyclic behavior of panel zone in beam-column subassemblies subjected to bidirectional loading, *Journal of Constructional Steel Research*, Vol.143, pp.32-45. 2018.4

[6] Namba, H., Tabuchi, M., and Tanaka, T.: Behavior of joint panels in chs column to beam connections, *Journal of Structural and Construction Engineering* (*Transactions of AIJ*), No.518, pp.95-102, 1999.4 (in Japanese)

[7] Hiura, H., Tabuchi, M., et al.: Elasto-plastic behaviour on column-to-beam joint panel under two direction share force, *Annual report of AIJ Kinki Branch*, No.43, Structural Division, pp.341-344, 2003.5 (in Japanese)

[8] AIJ: *Structural Steelwork specification for Building Construction JASS6*, Architectural Institute of Japan, 2018.1 (in Japanese)

[9] Mukaide, S., and Kuwahara, S.: Ductility demand of beams and joint panels in steel moment frames, *Journal of Structural and Construction Engineering* (*Transactions of AIJ*), Vol. 67, No.555, pp.163-170, 2002.5 (in Japanese)